A 3D Model Of A MHD Faraday Linear Generator

Author(s): A. Geri, A. Salvini, and G. M. Vecca

Session Name: Poster Papers

SEAM: 32 (1994)

SEAM EDX URL: https://edx.netl.doe.gov/dataset/seam-32

EDX Paper ID: 1712

A 3D Model of a MHD Faraday Linear Generator

A. Geri, A. Salvini and G.M. Veca, IEEE Senior Member
Dipartimento di Ingegneria Elettrica - Università degli Studi di Roma "La Sapienza"
Via Eudossiana, 18 - 00184 Roma (Italy)

ABSTRACT

n this paper the authors describe a 3D model for MHD Faraday inear generators which can be used as an alternative to the ntegration of Basic MHD set of equations (1). The main goal is to lefine a computational model capable of giving good results from the oint of view of the macroscopic behaviour of the plasma during the MHD energy conversion. The model is based on the partitioning of he ionized gas in an arbitrary number of small parallelepiped-haped volumes. In correspondence with each barycentre, the gasdynamic characteristic (velocity, pressure, conductivity, Hall arameter, etc.) has been evaluated by utilising experimental data nd by interpolating them with stationary curves available in heoretical studies. All these computed values are assumed as input lata, and the computational model uses them to evaluate the lectrical characteristics of the ionized gas. This approach, in unction with supplemental hypotheses, makes the authors able to epresent the energy conversion by an equivalent 3D lumped electric etwork in stationary regime. This circuit is composed of an lectrical resistive network excited by voltage sources representative f Faraday's law and Hall effects. Then, this network has been solved y means of node analysis and the macroscopic quantities having igh engineering interest such as output electrical power and load urrents have been computed. This approach permits to overcome all imitations due to the simulation of the non uniform gas discharge egime, which discouraged the development of 3D non-linear models olved in the time domain. Finally, the model has been validated by omparing numerical results against experimental tests executed on rototype Faraday generators.

INTRODUCTION

In the research on MHD energy conversion, the fundamental types of investigations are related to the characterization of the plasma discharge and the design of the device. On one hand, several analytical and experimental studies have been pointed out to investigate the plasma behaviour during the energy conversion. On the other hand, many computational models have been developed to support the designer activity during the optimization of the device performance. However, in both cases two important requirements must be satisfied: accuracy and feasibility of simulations. These exigencies are often in conflict. In particular, for computational models, the numerical precision can generally be obtained only by means of relevant investment of computer resources (time and memory). The difficult to develop a 3D model, which satisfies the exigencies previously cited, is greater than for two-, one- and zero-dimensional models. But it is important to note that in many technical cases a 3D model is fundamental for the correct evaluation of the performance of MHD devices. For examples[1] the present 3D model permitted the evaluation of the performance of the Faraday MHD generator varying the external 3D magnetic field map generated by a super-conductive (sc) magnet. As just said, there is not a relevant number of three-dimensional models while it is very common to find zero-, one- and two- dimensional ones expecially when analytical approaches are used. In fact in this case the basic set of MHD equations (1) must be simultaniously solved together with equation (2) which takes in to account electric and magnetic effects[2].

$$\delta\frac{\partial}{\partial t}\left(\frac{v^2}{2}+U+\frac{\varepsilon E^2}{2}+\frac{B^2}{2\mu_o}\right)+\delta\bar{v}\cdot\nabla\left(\frac{v^2}{2}+U\right)=-\nabla\cdot(\bar{v}p)-\nabla\cdot\left(\frac{\bar{E}\times\bar{B}}{\mu_o}\right)$$

$$\delta\left(\frac{\partial}{\partial t}+\bar{v}\cdot\nabla\right)\bar{v}=\bar{j}\times\bar{B}-\nabla\left(p-\frac{1}{3}\mu_v\nabla\cdot\bar{v}\right)+\mu_v\nabla^2\bar{v} \qquad (1)$$

$$\left(\frac{\partial}{\partial t}+\bar{v}\cdot\nabla\right)\delta=-\delta\nabla\cdot\bar{v}$$

where

$$\bar{j}=\sigma\bar{E}^*-\frac{\beta}{B}(\bar{j}\times\bar{B}) \qquad (2)$$

with

$$\bar{E}^*=-\nabla\bar{V}+\bar{v}\times\bar{B} \qquad (3)$$

The meaning of the symbols used above is:

δ	= mass density of fluid	[kg/m^3]
$\bar{v}$	= velocity	[m/s]
ε	= dielectric constant	[F/m]
E	= electric field	[V/m]
$\bar{B}$	= magnetic induction	[T]
μ_o	= magnetic permeability	[H/m]
p	= pressure	[N/m^2]
U	= internal energy of the gas	[J]
μ_v	= dynamic viscosity of fluid	[Ns/m^2]
t	= time	[s]
$\bar{j}$	= current density	[A/m^2]
$\bar{E}^*$	= total electric field	[V/m]
$\bar{V}$	= electric voltage	[V]
β	= Hall parameter	

The Hall parameter is defined by:

$$\beta=\omega\tau=\frac{eB}{m_e n Q c_e} \qquad (4)$$

where ω is the cyclotron frequency, τ is the average time between two electron collisions, c_e is the average velocity of thermal agitation, m_e is the electron mass, n is the atomic and molecular density, Q is the crossectional dimension from which the motion quantity transmission occurs and e is the electron electric charge. Moreover, in the energy conversion there are also other phenomena

which must be taken in account. In particular, one of the most relevant aspect is the nonuniform discharge regime. This phenomenon has been studied in many experimental and theoretical works[3,4,5]. Its simulation is very difficult because it is always necessary to introduce theoretical hypothesis on discharge evolution by means of hypothetical assumptions on arching characteristics or periodical variations of the plasma electrical conductivity. This time dependent evolution must be considered during the integration of the Basic MHD set of equations (1) to obtain a suitable description of the real physical phenomenon. But the difficulties are evident. However, it has been pointed out how in Faraday MHD generators the effects of the electrical nonuniformities are rather small[5]. In spite of this, the Basic MHD set of equations (1) can be integrated only by means of simplifying hypotheses both in gasdynamic and in electric terms. An example[6] of a 3D model based on the integration of parabolized Basic MHD set of equations (1) by means of Rational-Runge-Kutta methods for integrating in the main flow direction and Galerkin finite element method for integrating in each perpendicular cross-section has been just presented[6]. An alternative to this approach can be obtained by means of lumped electric circuit. The aim of this work is to describe a 3D circuital model capable to evaluate the performance of the MHD Faraday generator from a macroscopic point of view (more accurate investigation can be also pointed out increasing the computational resource investments). For this type of generator the nonuniformities can be neglected as previously said. This simplification allows to avoid the time domain analysis which requires a long time of computation. Consequently, in our model the energy conversion is studied using an equivalent stationary regime. In addition, under appropriate simplifying hypotheses, for Faraday generators, it is also possible to introduce a reduced set of equations to solve, in stationary condition, the equivalent electrical network. All these simplifications, which make the computation fast and reliable, are justified by experimental observations on prototype Faraday generators[5].

THE MODEL

General description

The proposed model is based on a circuit approach deduced from 2D models described in literature[3,4,7] and from the one developed by the authors[8] to simulate liquid metal MHD pumps by 3D equivalent electrical network. The plasma and the duct belonging to the active region (i.e. the section of the device where are located the electrodes and where the external magnetic field acts, see Fig. 1a) are subdivided in a finite number of elementary parallelepiped-shaped volumes (bricks) (see Fig. 1b). The precision degree of the model depends strongly on the number of elementary bricks. The sides of each brick are called A_x, A_y, A_z, while afterwards we will call l_{x-in}, l_{z-in} the dimensions of the inlet cross section of the channel, l_{x-out}, l_{z-out} the outlet cross section ones and l_y the active length along the y axis which is parallel to the velocity of the main flow of the plasma. The cross sectional side dimensions of the channel at a generic y coordinate will be indicated as l_{x-y}, l_{z-y}. These dimensions are variable along y axis, and the geometric relations to determinate them are:

$$l_{x-y} = \frac{l_{x-out} - l_{x-in}}{l_y} y + l_{x-out} \qquad (5)$$

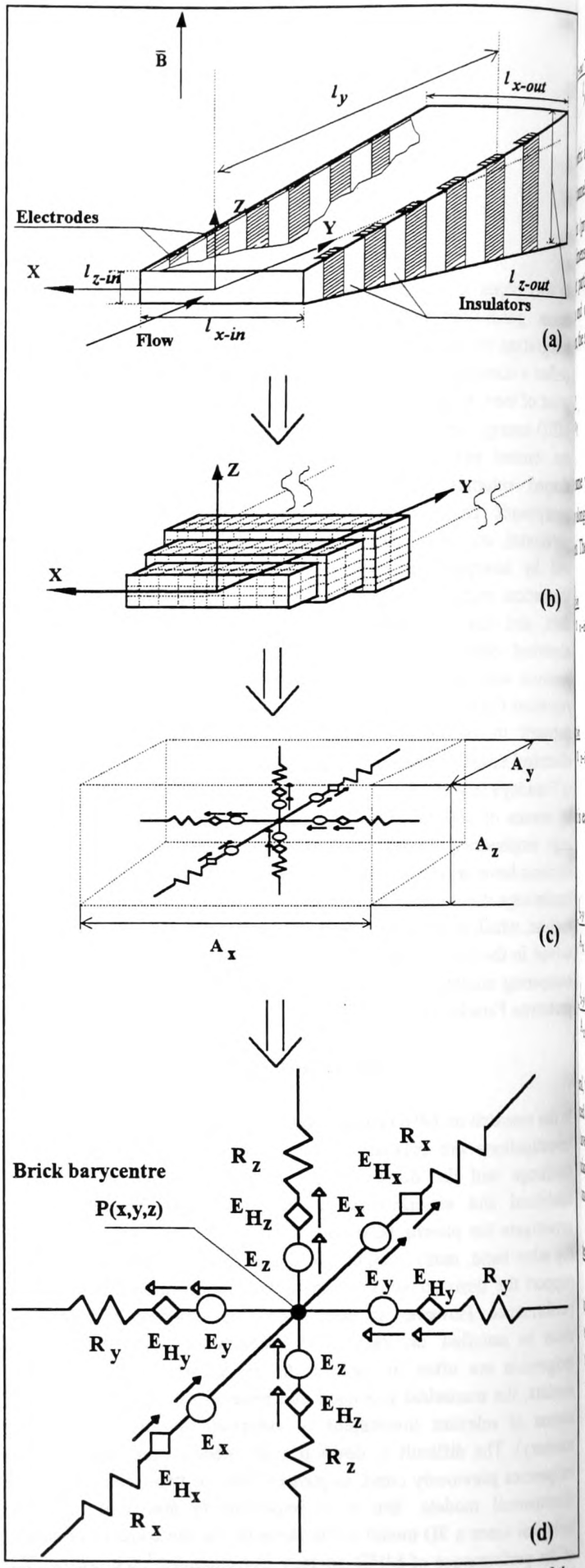

Fig. 1 - Modelling of MHD linear generators: a) active region of the MHD linear generator; b) plasma partitioning in elementary volume of parallelepiped shape; c) example of the equivalent electrical circuit associated to each elementary parallelepiped (brick); d) zoom of the electrical network of each brick.

nd

$$_{z-y} = \frac{l_{z-out} - l_{z-in}}{l_y} y + l_{x-out} \qquad (6)$$

A geometric algorithm provides to partition the active length of the MHD channel by a preliminary subdivision of the l_y length in n_y egments (preferably smaller than the inter-electrode insulating pace dimension or, alternatively, it is possible to operate two different partitions along y axis and, precisely, one for electrode egions and one for insulating regions). Referring to the simple artition, the side along the y axis of the elementary brick is:

$$_y = \frac{l_y}{n_y} . \qquad (7)$$

n the same way each cross section which has a surface growing inearly along the y axes, has been partitioned in $n_x(y)$ and $n_z(y)$ egments. The elementary brick sides along x and z axis are then:

$$_x = \frac{l_{x\text{-}in}}{n_{x-in}} \qquad (8)$$

nd

$$A_z = \frac{l_{z\text{-}in}}{n_{z-in}} . \qquad (9)$$

Now it is easy to determine the number of segments $n_x(y)$ and $n_z(y)$:

$$n_x(y) = \frac{l_{x\text{-}y}}{A_x} \qquad (10)$$

$$n_z(y) = \frac{l_{z\text{-}y}}{A_z} . \qquad (11)$$

In general, these formulae do not give integer numbers, thus we have introduced an approximation consisting of accepting all the bricks which have their barycentre internal to the duct. Then, it is possible to introduce the equivalent 3D electrical network of each brick (see Fig. 1c and Fig. 1d) .

Equivalent electrical network

The equivalent electrical network consists of a collection of lumped resistive dipoles and ideal voltage sources. The resistive components take into account the conductive phenomena within the ionized gas. The active components are of two types: independent voltage sources and current-controlled voltage sources. The ideal independent voltage sources take into account the emfs deriving from Faraday law. In fact the plasma can be assumed as a conductor flowing with a velocity $\bar{v}$ through an high magnetic field, $\bar{H}$. In this case, an electromotive force is induced in the plasma according to the well-known equation:

$$\bar{E} = \bar{v} \times \mu_o \bar{H} \qquad (12)$$

The ideal current-controlled voltage sources simulate the emfs within the plasma due to the Hall effect. This choice is justified by the fact that, as it will be more evident next, these emfs depend on the total magnetic field (i.e. the external magnetic field added to the reaction field) and on the spatial current distribution (i.e., the branch current in the equivalent electrical network of each brick). Temporally, to model each brick of the plasma, it is possible to assume that all main physical quantities, which play a relevant part in the determination of the electrical network parameters, are hypothetically known (the method to evaluate these values will be explained in a next paragraph). Under this assumption, the resistive parameters, the Faraday generators and the Hall generators are respectively given by:

$$R_i = \frac{1}{\sigma(x,y,z)} \frac{A_i}{2A_jA_k} \qquad (13)$$

$$E_i = \int \bar{v} \times \bar{B} \cdot d\bar{l} = \left[v_j H_k - v_k H_j \right] \frac{\mu_o A_i}{2} \qquad (14)$$

$$E_{H_i} = \int \bar{J} \times \bar{B} \cdot d\bar{l} = -\frac{\beta(x,y,z)}{\sigma(x,y,z)\left|\bar{H}\right|} \left[J_j H_k - J_k H_j \right] \frac{A_i}{2} \qquad (15)$$

with $i = x, y, z$, $j = y, z, x$ and $k = z, x, y$

$$d\bar{l} = dx\bar{g}_x + dy\bar{g}_y + dz\bar{g}_z .$$

The spatial distributions $\sigma(x,y,z)$ and $\beta(x,y,z)$ represent the conductivity and the Hall parameter (as scalar quantities) evaluated in correspondence with the barycentre of the brick, while $\bar{v}(x,y,z)$, $\bar{H}(x,y,z)$, $\bar{J}(x,y,z)$ are the spatial distributions of the vectors velocity, of the total magnetic field and of the current density. For this last distribution we have assumed that each component is given by:

$$J_i(x,y,z) = \frac{I_i(x,y,z)}{A_jA_k} \qquad (16)$$

where I_i is the current flowing along the i axis and A_j and A_k are the above defined edge lengths of plasma bricks. The last elements to define are the resistances able to simulate the electrodes, the insulating walls and the electric loads.

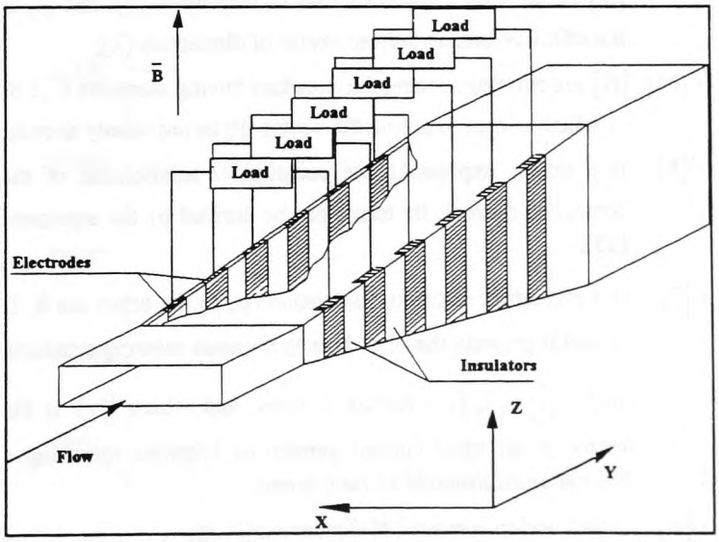

Fig. 2 - MHD Faraday linear generator: each electric load is subject to Faraday emf.

The resistances of electrodes and insulating walls can be easily derived take in mind the electrical characteristics of these materials. In particular, when the calculation has not to compute the wall electrical losses, it is possible to introduce a relevant simplification by assigning the resistivity $\rho_e = 0$ to the electrodes and the resistivity $\rho_i = \infty$ to the insulating walls. The electric loads are instead input data and their connection with the electrodes determine the different types of MHD linear generators. For the Faraday generator the load resistances are linked at each electrode pair located perpendicularly with respect to the gas flow axis (y axis, see Fig. 2).

Network analysis

Performing opportune transformations on each serial branch which links two adjacent brick barycenters, we can obtain an equivalent electrical network having n nodes:

$$n = n_b + n_e \tag{17}$$

where n_b is the number of the bricks and n_e is the number of electrodes. This network can be solved by means of node analysis[10,11,12]. In this case the basic equations to solve are:

$$[I_{no}] = [G_{no}][V_{no}] \tag{18}$$

where $[I_{no}]$ is the column vector of the node current sources, $[G_{no}]$ is the node conductance matrix and $[V_{no}]$ is the column vector of the unknown nodal electric potential. The dimension of this system is $\xi = n - 1$, where n has been defined above. The structure of the system must be modified to introduce the current-controlled voltage sources. In general, dependent sources can be taken into account by means of additional set of $\varphi \le \lambda$ equations, where λ is the number of the electric branches of the network. In this case the node method permits to write the following system of equations:

$$[P] - [N][T_p]^T[F][P] - \{[M] - [N][G^*]\}[A]^T[V_{no}] = [N][I'] \tag{19}$$

where:

- $[P]$ is the vector containing the branch current piloting the controlled sources defined by $[P] = [M][V] + [N][I]$; where $[V]$ is the branch voltage vector of dimension (λ); and $[I]$ is the effective branch current vector of dimension (λ);
- $[M]$, $[N]$ are suitable rectangular matrices having elements 0 ,1 or -1 which permit to define the vector [P] as previously shown;
- $[F]$ is a matrix expressing the constitutive relationship of the controlled sources, its terms can be derived by the equations (15);
- $[T_p]$ is a projection matrix of dimension (φ, λ); its terms are 0, 1, -1 and it projects the pilot branch currents creating a column vector $[\hat{I}] = [T_p][I_0]$ having λ rows, and where $[I_0]$ is the vector of all ideal current generators obtained operating a Norton transformation of each branch;
- $[A]$ is the incidence matrix of dimension (λ, ξ);
- $[G^*]$ is a diagonal matrix of dimension (λ, λ); its terms are the branch conductances and it is linked to the node conductance matrix by: $[G_{no}] = [A][G^*][A]^T$;
- $[I']$ is a column vector obtained by cancelling in $[I_0]$ all the rows in which a controlled source is present.

Systems (18) and (19) must be simultaneously solved and the total set of equations has $\xi + \varphi$ dimension. From the analysis of the equivalent electrical circuit of each brick (see Fig. 1d) one can easily note that all branches of the network have a dependent source. Thus, for practical plasma partitioning, the dimension $(\xi + \lambda + n_e / 2)$ of the total set of equations is unacceptable because, also using appropriate sparse matrix algorithms, the computational time can be too high. Successfully in Faraday generators a relevant number of simplifications can be introduced. In fact in this special case, the current mainly flows along the x axis direction where the discharges take place and the emfs given by (12) are present (see Fig. 1). For these reasons it is possible to assume $\bar{J}(x,y,z) \cong J_x(x,y,z)\bar{g}_x$. In addition, considering $\bar{H}(x,y,z) \cong H_z(x,y,z)\bar{g}_z$ and $\bar{v}(x,y,z) \cong v_y(x,y,z)\bar{g}_y$, (14) and (15) become:

$$E_x = v_y \mu_o H_z \frac{A_x}{2} \tag{20}$$

$$E_{H_y} = \int \bar{J} \times \bar{B} \cdot d\bar{l} = -\frac{\beta(x,y,z)}{\sigma(x,y,z)\left|\bar{H}\right|} J_x H_z \frac{A_y}{2} \tag{21}$$

That is, in our model are only present ideal voltage sources (that act along the x axis according to (20)) and ideal current-controlled sources (that act along the y axis according to (21)). Consequently, the set of equations given by (18) and (19) can be simplified as described below. The $[G_{no}]$ matrix can be subdivided into the sum of two sub-matrices:

$$[G_{no}] = [G'] + [G''] \tag{22}$$

where [G'] is the simple conductance matrix without considering the controlled source, while [G''] is the matrix which takes into account only by the elements due to the controlled sources. The matrix [G'] is symmetric and its mutual and diagonal terms G'_{rr} and $G'_{r,s}$ are expressed by:

$$G_{r,s} = -\left(\frac{1}{\sigma(x_r,y_r,z_r)} + \frac{1}{\sigma(x_s,y_s,z_s)}\right)\frac{A_i}{2A_jA_k} \tag{23}$$

$$G_{r,r} = \sum_s -G_{r,s} \tag{24}$$

where (x_r, y_r, z_r) and (x_s, y_s, z_s) are the coordinates of the r^{th} and s^{th} node which are respectively coincident, as shown before, with the barycentres of two neighbour bricks; the summation in (24) is extended to all branches of the r^{th} node. The [G''] matrix is easy determinable[10] as follows:

$$G''_{l,p} = G''_{m,q} = +C_c \tag{25}$$

and

$$G''_{m,p} = G''_{l,q} = -C_c \qquad (26)$$

where l and m are the generic row indices while p and q are the generic column indices of the [G"]. Precisely, between the nodes l and m there is the current-controlled voltage source, while between p and q nodes there is the branch in which the piloting current will be found. Because we have only current-controlled voltage sources, all branches between neighbouring nodes must be transformed according to the Norton representation and at the same time the controlling quantity from effective current branch to equivalent voltage E_c. By operating in this way the term C_c can be easily reduced. Similarly the $[I_{no}]$ can be obtained[10] as the sum of two column-vectors:

$$I_{no}] = [I]+[I''']. \qquad (27)$$

where

$$''_l = - C_c E_c \qquad (28)$$

and

$$''_m = + C_c E_c \qquad (29)$$

while the column-vector [I'] can be written in the usual way. By using this approach we have obtained a system of equation of dimension ξ. But in this case the sparsity of the matrix $[G_{no}]$ is reduced and, in general, the symmetry is compromised.

IONIZED GAS CHARACTERIZATION

General considerations

The evaluation of the main physical quantities is a fundamental problem in MHD generator modelling. Many theoretical, experimental and empirical studies have been proposed and a lot of models have been developed to simulate MHD generators from a microscopic point of view. This approach permits a partial or total estimation of all unknown physical quantities during the simulation of the energy conversion. All models developed using this method are very attractive, because the physical phenomenon is entirely simulated. However, their implementation in a calculation code presents difficulties not easily surmountable. In addition, these models are strictly dependent from the particular generator under analysis (i.e., they are implemented referring to specific plasma characteristics, assigned load interconnections and so on). Consequently, the generalization of their use to every realistic device arrangement is not a trivial problem. For all these reasons, the application of these models, during the preliminary design phase of generator devices, is inadequate. In fact, the designer needs of a generalized and flexible code able to provide fast and reliable results for every configuration to analyse. This goal can be matched by a macroscopic model of the device. In this case, using appropriate strategies, the physical quantities can be computed separately from the computational MHD generator model. Probably, their evaluation will be affected by a relevant degree of uncertainty, but it can be made independently from the particular device under analysis. Thus, the generality of the code is obtained and the rapidity of the computations is ensured. The model proposed in this paper has been developed using this method. In order to evaluate all parameters of the equivalent electrical network described, it is necessary to introduce as input data the conductivity, the Hall parameter, the velocity and the magnetic field which characterize the specific MHD energy conversion under analysis. These values can be extrapolated merging theoretical and experimental studies available in literature as described below.

Temperature and pressure distribution

From the analysis of many experimental data[8, 14] we have observed that:

- along the channel the temperature, T(0,y,0), has a decreasing trend from its maximum value, in correspondence with the inlet cross section, T(0,0,0), to its minimum value, in correspondence with the outlet cross section, $T(0,l_y,0)$ (this distribution, which may be considered linear, is shown in Fig. 3);
- on the cross section, the gas flowing in the duct has its maximum temperature value, T_{cc}, in the central core of the channel (hot region), while it has its minimum value near the walls (boundary layer); for practical case, an estimation of this values can be fixed by:

$$T_w = \gamma T_{cc} \qquad (30)$$

with $\gamma = 0.5 \div 0.9$.

Observing that on the cross section the representative curve of the temperature evolution (see Fig. 4) is the same either along the x axis or the z axis, one can easily determine a 3D distribution of the temperature inside the plasma combining the curves plotted in Fig. 3 and Fig. 4. This function is given by:

$$\begin{cases} T(x,y,z) = T(y)\cdot e^{\frac{\ln\gamma}{(L'L''-x^2z^2)}\left[(L''^2-z^2)x^2+(L'^2-x^2)z^2\right]} \\ \qquad\qquad \text{for} \quad -L' < x < L' \qquad -L'' < z < L'' \\ T(\pm L', y, \pm L'') = \gamma T(y) \end{cases} \qquad (31)$$

with $L' = \frac{l_{x-y}}{2}$ $L'' = \frac{l_{z-y}}{2}$

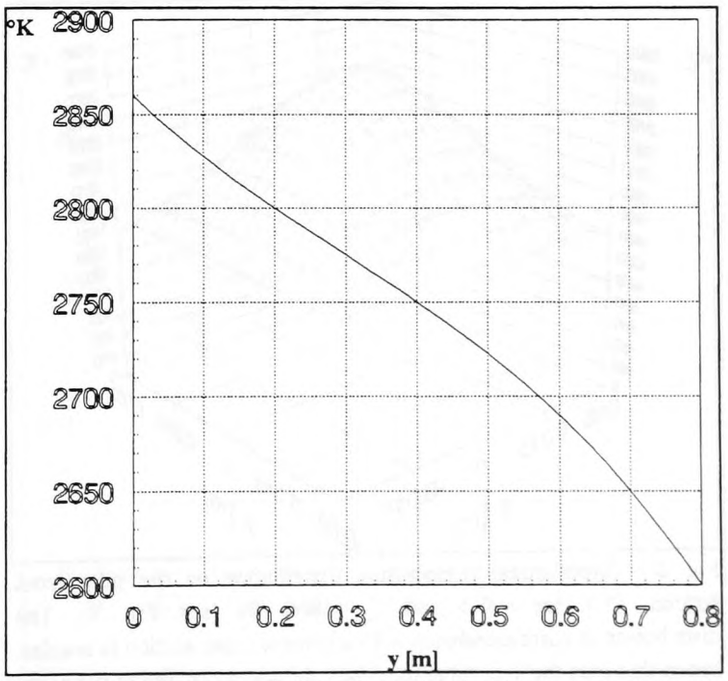

Fig. 3 - Temperature evolution along the channel axis as deduced from experimental data[8].

and assuming the following set of boundary conditions:

$$\begin{cases} T(\pm L', y, z) = T(x, y, \pm L'') = \gamma T(y) = \gamma T_{cc} \\ T(0, y, 0) = T(y) = T_{cc} \end{cases}$$

In Fig. 5 T(x,y,z) the temperature distribution corresponding to the inlet cross section, T(x,0,z), is shown.

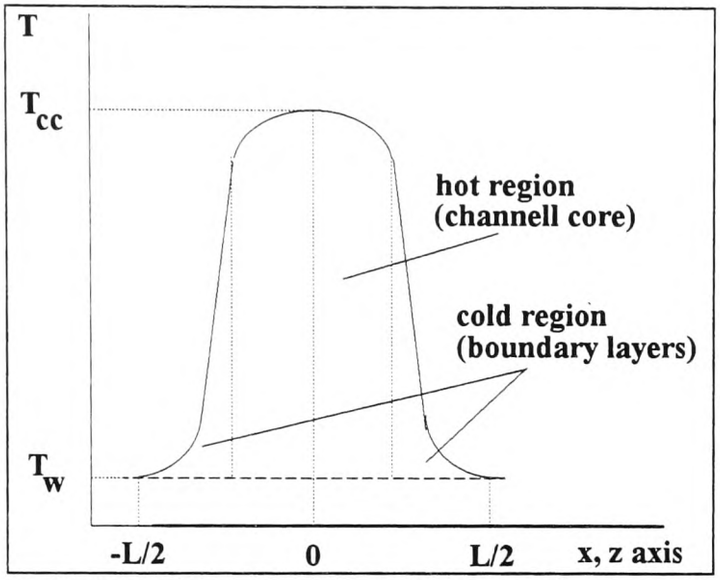

Fig. 4 - Hypothetical temperature trend corresponding to a generic cross section of the duct. By imposing the thermal equilibrium near the walls, the plasma must have the same temperature of the inner walls, T_w. This distribution has been simulated by a Gauss' curve where:

T_{cc} is the temperature along the channel axis;
T_w is the inner walls temperature;
L is the transversal dimension of the generic cross section of the channel.

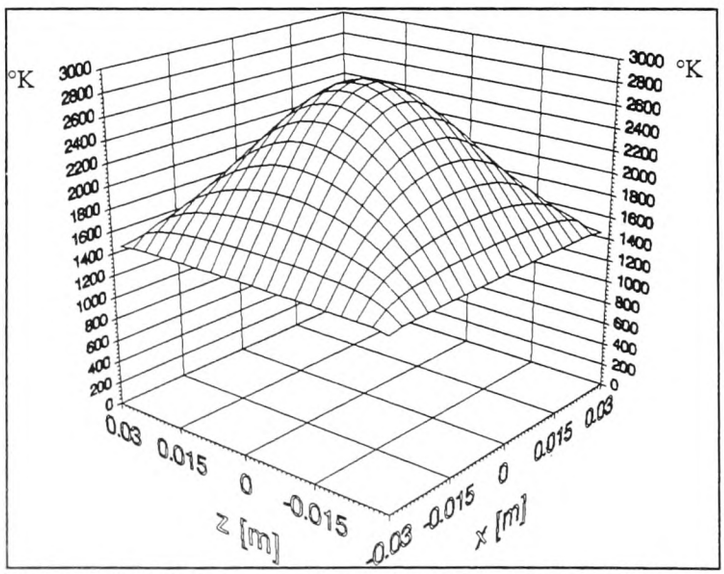

Fig. 5 - Hypothetical temperature distribution on the inlet cross section, y=0, for γ=0.5 and T_{cc}=2860 °K (see Fig. 3). The distribution in correspondence with a generic cross section is similar, but in this case the T_{cc} value must be changed according to the curve plotted in Fig. 3.

Similarly, considering the following polytropic transformation:

$$p(x,y,z) = p(y)\left(\frac{T(x,y,z)}{T_{cc}}\right)^m \qquad (32)$$

where m is a suitable empirical coefficient, it is possible to suppose a pressure distribution inside the plasma, p(x,y,z). As for the temperature, the pressure distribution along the channel axis, p(y), can be deduced from experimental measurements.

Conductivity and Hall parameter evaluations

Temperature distribution, T(x,y,z), jointly with pressure distribution p(x,y,z), can be advantageously used to estimate hypothetical spatial distributions of plasma conductivity and Hall parameter. In fact, in many empirical[6] and theoretical[2] studies available in literature, the conductivity and Hall parameter versus temperature and pressure are plotted in stationary regime. Thus, among all these graphics, it is possible to choose the curves which correspond to the specific device under analysis. For examples, referring to the device tested by Ehindhoven Blow Down Facility[3, 4, 9] (used to validate our model), we select the calculated curves in stationary regime pertinent to Argon seeded by Cesium[2]. From the analysis of these curves, it is possible to deduce that plasma conductivity is greatly variable with temperature. At the same time, the conductivity is substantially invariant with pressure, thus it is sufficient only one curve to represent this dependence[2] (e.g., the curve at 1 atm pressure). In addition, observing that in MHD conversions typical working temperatures are in the range 2000 ÷ 3000 °K, inner to these limits the theoretical curve chosen[2] can be easily interpolated by means of a polynomial function (see Fig. 6), obtaining:

$$\log \sigma = aT^2 + bT + c \qquad (33)$$

where a, b and c are opportune coefficients. For Argon seeded with Caesium they assume the values:

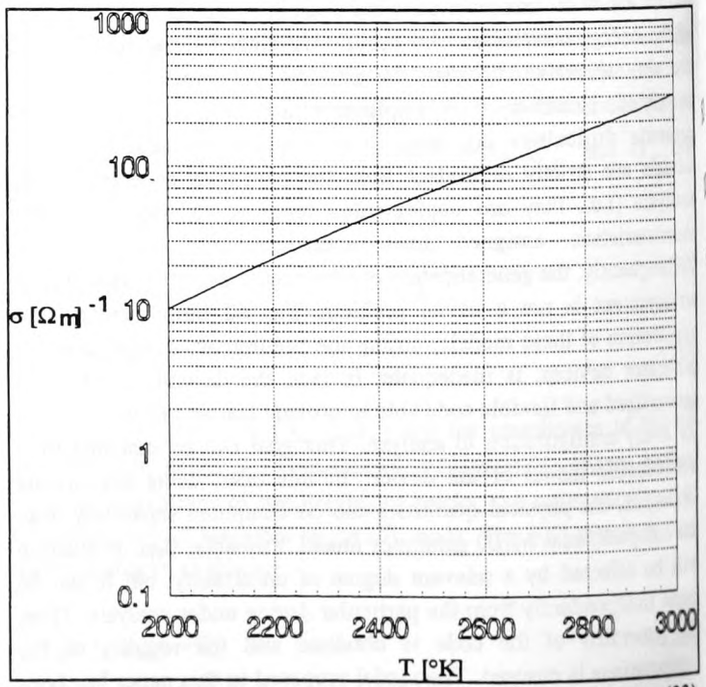

Fig. 6 - Conductivity evolution versus temperature according to (33) for Argon seeded with Caesium.

$a = -3.486 \cdot 10^{-7} \quad \left[\Omega^{-1}m^{-1}K^{-2}\right]$

$b = 3.22 \cdot 10^{-3} \quad \left[\Omega^{-1}m^{-1}K^{-1}\right]$

$c = -4.046 \quad \left[\Omega^{-1}m^{-1}\right]$

Introducing (31) in (33), the desired hypothetical spatial distribution of the plasma conductivity, $\sigma(x,y,z)$, can be obtained. For the inlet cross section this distribution is drawn in Fig. 7. This approach permits to overcome all difficulties linked to the evaluation of the conductivity distribution as suggested in previous studies[8, 13]:

$$\sigma = \Psi J^{\theta} \tag{34}$$

in which J is the current density while Ψ and θ are parameters variable with generator characteristics (e.g., they depend from plasma used, thermodynamic conditions, load interconnections and so on).

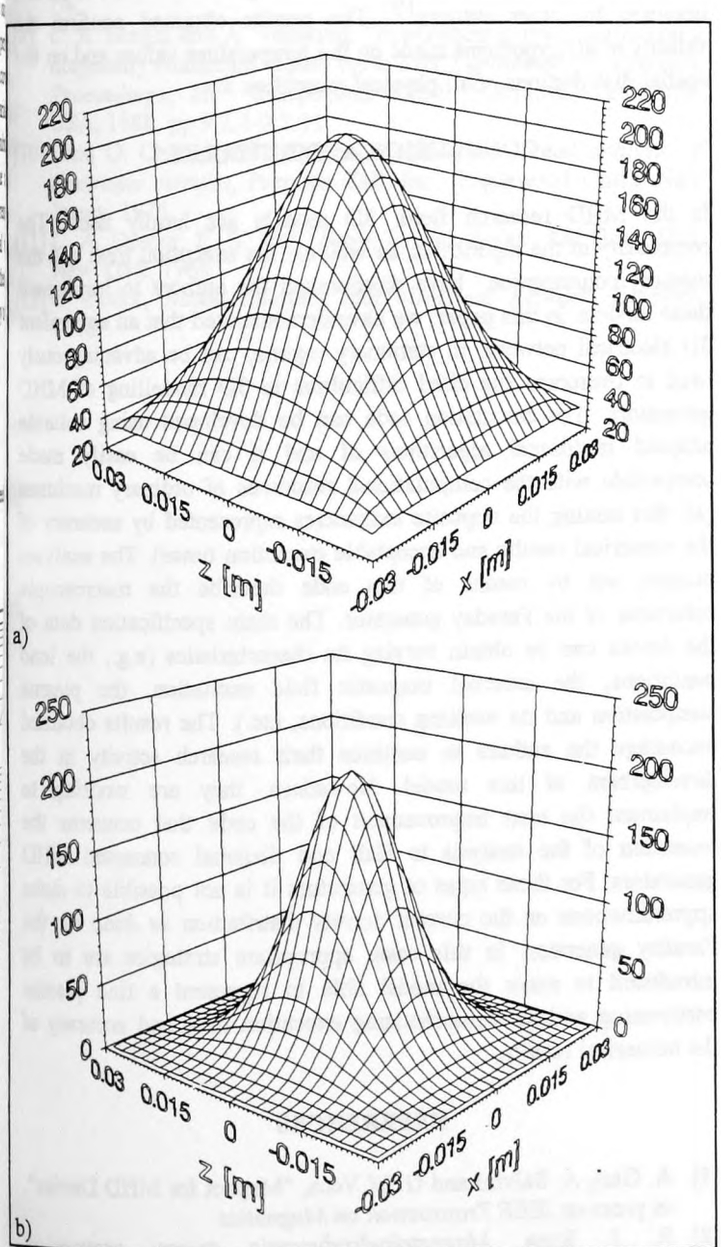

Fig. 7 - Conductivity distribution corresponding to the inlet cross section for Argon seeded with Cesium: a) $\gamma = 0.8$; b) $\gamma = 0.5$. The conductivity v...

Equation (34) makes the simulation model of non linear type, consequently it must be solved in the time domain and its execution becomes critical and slow. Working as previously described, the distribution of Hall parameter, $\beta(x,y,z)$, can be also deduced. In particular, by analysing theoretical distributions[2] in stationary regime, one can note that β is strongly influenced both by temperature values and by pressure values. But in this case, theoretical and empirical curves[8] shown that, as first approximation, it is possible to make a reasonable simplification by considering the Hall parameter as only temperature function. On the base of this assumption, we can only consider the theoretical curve[2] corresponding to the averaged pressure value of 1 atm. An example of Hall parameter distribution along the channel axis is plotted in Fig. 8.

Velocity and magnetic field distributions

The usual working conditions of the plasma flowing in MHD generators are characterised by a turbulence regime. For this reason, we have considered a constant gas velocity along the channel. Thus, this distribution can be simulated as a vector having a constant modulus with versus and direction coincident with the y axis:

$$\bar{v}(x,y,z) \cong v_Z(x,y,z)\bar{g}_Z \cong v_Z\bar{g}_Z \tag{35}$$

The simulation proposed below (executed with the aim to validate our model) has been carryed out on the base of this simplificative ipothesis, because no specific characteristics were availabe on magnet used during the experimental tests[3]. Other 3D spatial distributions can be computed without difficulties introducing appropriate working hypotheses and boundary conditions, as described in previous papers[8, 18]. The magnetic field map can be obtained using general purpose code (such as GFUN or ANSYS) based on integral or finite element method. This map can be easily evaluated varying the magnet shape (i.e. prototype, cylindrical saddle, rectangular saddle, dipoles modular magnet, etc.[1, 15, 16, 17, 18]), obtaining the desired 3D distribution of the magnetic field:

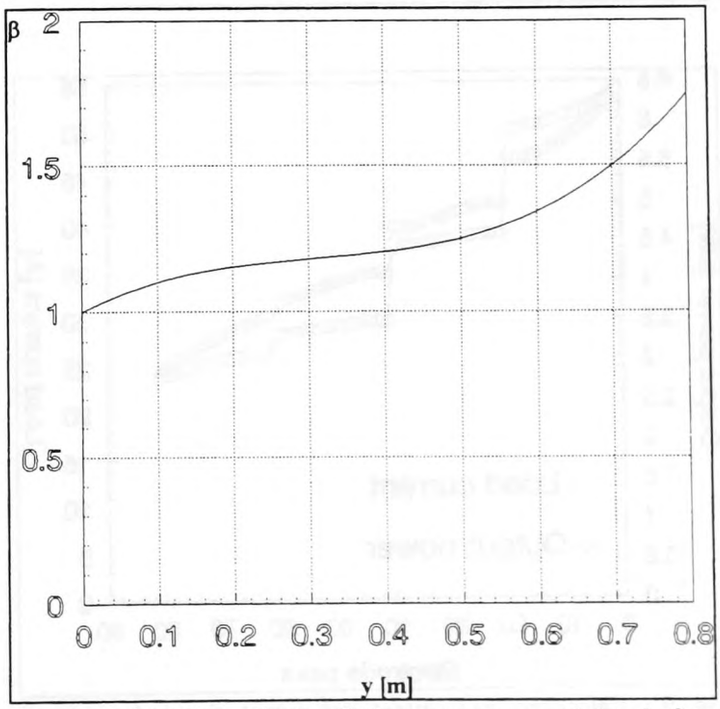

Fig. 8 - Evolution of the Hall parameter as deduced from experimental tests[3].

$$\bar{H}(x,y,z) = H_X(x,y,z)\bar{g}_X + H_Y(x,y,z)\bar{g}_Y + H_Z(x,y,z)\bar{g}_Z \qquad (36)$$

Often, the magnetic field map distribution can be considered uniform inside the active region, thus (36) can be simplified assuming, as first approximation, the magnetic field vector having a constant H_Z component only:

$$\bar{H}(x,y,z) \cong H_Z(x,y,z)\bar{g}_Z \cong H_Z\bar{g}_Z \qquad (37)$$

The simulation proposed below (executed with the aim to validate our model) has been carryed out on the base of this simplificative ipothesis, because no specific characteristics were availabe on magnet used during the experimental tests[3].

MODEL VALIDATION

The model proposed in this paper has been validated using experimental data[3]. In Table I we have summarised the main characteristics of the device tested, the measured output power, the hypothetical temperature values and the computed output power.

TABLE I

EXPERIMENTAL DATA AND COMPUTATIONAL VALUES

Description	Value
Inlet / Outlet section	60×60 / 120x120 mm^2
Velocity	1200 m/s
Active length	0.80 m
Magnetic induction	2.5 T
Number of electrode pairs	81
Load resistances	$R_{1\text{-}15} = 2.2\ \Omega$ $R_{16\text{-}35} = 3.3\ \Omega$ $R_{36\text{-}59} = 4.7\ \Omega$ $R_{60\text{-}81} = 5.1\ \Omega$
Plasma flowing in the MHD channel	Argon + $2x10^{-4}$ Cesium
Measured output electric power	380 kW
Inlet / Outlet temperature	2860 / 2600 K
Wall temperature	0.5 · axis value
Computed output electric power	360.6 kW

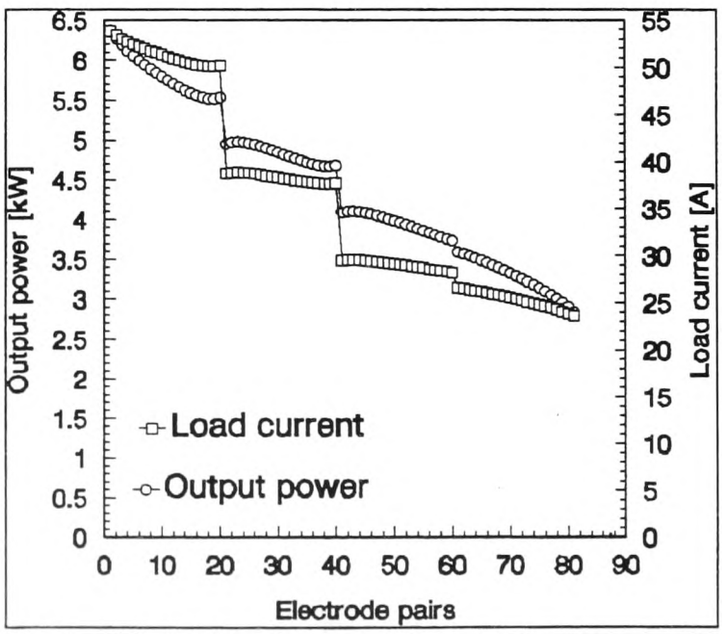

Fig. 9 - Calculated load current and output electrical power in correspondence with each electrode pair.

We underline that the inlet/outlet temperature, as well as the wall temperature, have been chosen in agreement with the standard values proposed in literature[2]. The simulation has been executed using the spatial distributions of all physical quantities previously determined. The plasma partitioning used for this simulation is not so high as an accurate evaluation should require. We have make this choice to reduce the number of equations and thus to obtain a smaller computational time (developing appropriate LU factorization scheme for structurally symmetric sparse matrix, it would be possible to optimize the solution of the system with a relevant reduction of the time required for the calculations, and then it would be possible to thicken the plasma partitioning; however, nowadays this improvement has been not yet developed, even if we think to implement it in the next version of the code). But this fact has caused a reduction of the output power computed (we have verified that increasing the plasma partitioning, the output power tendentially grow up when the numerical stability of the solution has been not yet reached). In spite of this, it is interesting to note that the difference between the measured and the computed electrical power is very small (≅ 5%). In addition, as it is easy to note, the trend of the current along the y axis (see Fig. 9) is in agreement with the results obtained by other authors[19]. The results obtained confirm the validity of all hypothesis made on the temperature values and on the spatial distributions of all physical quantities.

CONCLUSION AND REMARKS

In the MHD research field, 3D models are hardly used. The complexity of the algorithms, as well as, the execution time and the memory consumption have discouraged the authors to implement these models. In this paper, we have demonstrated that an equivalent 3D electrical network, in stationary regime, can be advantageously used to overcome the cited difficulties in 3D modelling of MHD generators. The calculation code can be developed using suitable adapted traditional algorithms of and it can be easily made compatible with the computational resources of ordinary machines (all this mixing the opposite exigencies represented by accuracy of the numerical results and acceptable execution times). The analyses pointed out by means of this code describe the macroscopic behaviour of the Faraday generator. The main specification data of the device can be obtain varying its characteristics (e.g., the load conditions, the external magnetic field excitation, the plasma composition and its working conditions, etc.). The results obtained encourage the authors to continue their research activity in the development of this model. Nowadays, they are working to implement the next improvement of the code that concerns the extension of the analysis to Hall and diagonal connected MHD generators. For these types of generators it is not possible to make approximations on the current density distribution as done for the Faraday generator. In this case, appropriate strategies are to be introduced to make the model able to represent a fine plasma partitioning without compromising execution time and accuracy of the numerical results.

REFERENCES

[1] A. Geri, A. Salvini and G. M.Veca, "Magnet for MHD Device", in press on *IEEE Transaction on Magnetics*

[2] R. J. Rosa, *Magnetohydrodynamic energy conversion*, Hemisphere Publishing Corporation, Washington, 1987.

[3] C. A. Borghi, "Simulazione delle disuniformità della scarica elettrica in un generatore MHD a geometria lineare", *L'Energia Elettrica*, N. 3, 1989, pp. 97-102.

[4] C. A. Borghi and P. L. Ribani, "Network analysis of a noble gas MHD generator operating in the non-uniform discharge regime", *Conference Proceedings*, 10th International Conference on Electric Power Generation, Tiruchirapalli, India, December 1989, pp. XII.1-XII.6.

[5] M. Ishikawa, K. Kishimoto, S. Fukutomi and J. Umoto, "Simulation of electrical nonuniformities in diagonal type MHD generators", *Energy Conversion Mgmt.*, Vol.27, No. 2, pp. 261-265, 1987.

[6] M. Ishikawa and J. Umoto, "New Approach to Calculation Three-Dimensional Flow in MHD Generators", *Conference Proceedings*, 22nd Symposium EAM, Starkville, Mississippi, USA, 1983, pp. 2.8.1-2.8.17.

[7] C. A. Borghi, A. Massarini, G. Mazzanti and P. L. Ribani, "One- and Two-dimensional Models for a Linear MHD Generator Channel Design", *Plasma Devices and Operation*, Vol. 2, No. 2, 1992, pp. 125-139.

[8] A. Geri, G. M. Veca, "A three-dimensional lumped parameter model for MHD devices", *Conference Proceedings*, International Symposium on Electromagnetics field in Electrical Engineering ISEF '91 - September 18-20 1991, Southampton, UK.

[9] C. A. Borghi and A. Veefkind, "Experimental investigation on a diagonally connected closed cycle MHD generator", *Conference Proceedings*, 26th Symposium EAM, Nashville, Tennessee, USA, 1988, pp 9.2.1-9.2.11.

[10] Leon O. Chua and Pen-Men Lin, *Computer-aided analysis of electronic circuits*, Prentice-Hall, Inc., Englewood Cliffs, New Jersey, 1975.

[11] C. A. Desoer, E. S. Kuh, *Basic circuit theory*, Mc Graw Hill, New York, 1969.

[12] G. Fodor, *Nodal analysis and electrical network*, Elsevier, 1988.

[13] P. Massee et al., "The relation between the electrical conductivity and the current density in an MHD generator", Conference Procedeengs, 23rd Symposium on EAM, p.439, Somerset (Penn.), 1985.

[14] J. M. Wetzer, "Microscopic and Macroscopic Streamer Parameters of a noble gas linear MHD Generator", *Conference Proceedings*, 22nd Symposium EAM, Starkville, Mississippi, 1984, pp. 7.7.1-7.7.18.

[15] L. Cornaggia, C. Luzzatto and A. Manella, "MHD Power Plants: Requirements for the Superconducting Magnets and Electromagnetic and Structural Evaluation of the Design Concept of the Prototype and Demonstrative Magnet", *Conference Proceedings*, International Workshop on MHD Superconducting Magnets, Bologna November 13-15, 1991 Italy, pp. 1-8.

[16] G. M. A. Lia, I. Montanari and P. L. Ribani, "Design of Superconducting MHD Saddle Shaped Magnet Using an Optimization Procedure", *Conference Proceedings*, International Workshop on MHD Superconducting Magnets, Bologna November 13-15, 1991 Italy, pp. 9-13.

[17] G. Drago, A. Manella, P. Molfino, M. Repetto and G. Secondo, "Analysis and Design of Magnets for Linear and Disk MHD Applications", *Conference Proceedings*, International Workshop on MHD Superconducting Magnets, Bologna November 13-15, 1991 Italy, pp. 65-74.

[18] A. Geri and G. M. Veca, "Edge and Transient Effects Due to the SC Magnet in a MHD Device", *Conference Proceedings*, International Workshop on MHD Superconducting Magnets, Bologna November 13-15, 1991 Italy, pp. 59-64.

[19] C. A. Borghi, F. Negrini and P. L. Ribani, "Mathematical modeling for the channel design of a combustion plasma generator", *Conference Proceedings*, International Workshop on MHD Superconducting Magnets, Bologna November 21-23, 1990 Italy, pp. 185-194.